VIRTUAL WIND TUNNEL METHOD FOR PROJECTILE AERODYNAMIC CHARACTERIZATION

Paul Weinacht[1]

[1]*US Army Research Laboratory, Aberdeen Proving Ground, MD 21005-5066*

A numerical approach for completely characterizing the aerodynamic and flight dynamic performance of small caliber ammunition has been developed. The basis of the technique is two simple experiments which are performed in a virtual environment using a sophisticated computational fluid dynamic approach. The first experiment is the Magnus experiment where a spinning projectile is held at a fixed incidence to the oncoming flow. The second experiment is the pitch-damping experiment where the projectile is subjected to a prescribed motion that excites the angular rates associated with the pitching motion. Each experiment produces a different subset of the required aerodynamics, although both experiments can individually provide assessment of the static aerodynamics such as drag and gyroscopic stability. The combined results provide a complete assessment of the aerodynamic stability and performance.

INTRODUCTION

The assessment of the free-flight performance and stability of projectiles requires the determination of the complete set of static and dynamic aerodynamic coefficients. Much of the prior work has focused on the prediction of a subset of the complete aerodynamics, typically just the static aerodynamics. However, it is now possible to predict the complete set of aerodynamics for projectiles using two simple numerical experiments. The first experiment is the Magnus experiment where a spinning projectile is held at a fixed incident to the oncoming flow. The second experiment is the pitch-damping experiment where the projectile is subjected to a sinusoidal pitching motion or alternatively, a coning motion. Each experiment produces a different subset of the required aerodynamics, although both experiments can individually provide assessment of the static aerodynamics such as drag and gyroscopic stability. The combined results provide a complete assessment of the aerodynamic stability and performance. Although these experiments could be conducted in a wind tunnel, they are implemented here as a virtual environment analog via modern computational fluid dynamics techniques. The approach is different than virtual “fly-out” techniques, which

mimic the experiments typically performed in an aerodynamic range facility. While providing the same physical fidelity as the virtual fly-out approach, the virtual wind tunnel approach is as much as 100 to 1000 times more efficient.

The technique has been used to obtain important advances in the understanding of the flight dynamics of small caliber ammunition. One important area of focus is the trim angles often observed in low supersonic flight. These trim angles are normally associated with a nonlinear Magnus behavior, although both the Magnus and pitch-damping must be determined to predict the magnitude of the trim angle. The exact physical cause of these trim angles appears to be unexplained. The current approach is perfectly suited to examine this problem. In the past, it has been proposed that the rifling grooves may be a significant contributor to the nonlinear Magnus behavior. The current predictive methodology has shown that these effects are small for 5.56mm ammunition. However, the results do show that the rounded projectile base geometry from the manufacturing process contributes significantly to the nonlinear Magnus characteristics that result in trim angles. The approach is further used to demonstrate that a reasonable manufacturing change can be implemented, which completely eliminates the nonlinear Magnus and the trim angles at low supersonic velocities.

AERODYNAMIC MODEL

The form of aerodynamic models used to describe the flight mechanics of spinning projectiles is relatively well established. With the form of the model established, the role of the aerodynamicist is to populate these aerodynamic models with the necessary data so that the stability, performance, and free-flight motion can be predicted. For example, the transverse force and moment are shown below.

$$C_Y + iC_Z = -(C_{N_\alpha} + i\frac{pD}{V}C_{N_{p\alpha}})\tilde{\xi} - (C_{N_q} + C_{N_{\dot{\alpha}}})\tilde{\xi}' \quad (1)$$

$$C_m + iC_n = (i\frac{pD}{V}C_{M_{p\alpha}} - iC_{M_\alpha})\tilde{\xi} - i(C_{M_q} + C_{M_{\dot{\alpha}}})\tilde{\xi}' \quad (2)$$

The transverse force and moment contain contributions from the static normal force and pitching moment slopes C_{N_α} and C_{M_α}, the Magnus force and moment $C_{N_{p\alpha}}$ and $C_{M_{p\alpha}}$, and the pitch-damping force and moment $C_{N_q} + C_{N_{\dot{\alpha}}}$ and $C_{M_q} + C_{M_{\dot{\alpha}}}$ and are functions of the complex yaw $\tilde{\xi}$, yawing rate $\tilde{\xi}'$ and non-dimensional spin rate pD/V. In some applications, the Magnus force and the pitch-damping force are ignored because their contribution to the free-flight motion is small. For the same reason, these coefficients are also very difficult to measure in aeroballistic range facilities. Although their effect on the free-flight motion is small, the Magnus force and the pitch-damping force are required to recompute the respective moment coefficients if the center of

gravity varies from the baseline configuration. However, the current method provides the accurate determination of these coefficients as a by-product of the prediction of the Magnus moment and pitch-damping moment and allows these coefficients to be included in the aerodynamic model for completeness. The pitch-damping force and moment sum used in the aerodynamic models above are actually the sum of two independent aerodynamic coefficients/effects. For the nearly rectilinear motion experienced by most projectiles, the angular rates q and $\dot{\alpha}$ are nearly equal and the effect of angular rate on the aerodynamics can be treated as a single coefficient sum. Methods exist for independently determining these coefficients [1] and could be incorporated within the virtual wind tunnel method, although this is not warranted for the current application.

The aerodynamic model for the longitudinal force and moment is presented below.

$$C_X = -C_A \tag{3}$$

$$C_l = \frac{pD}{V} C_{L_p} \tag{4}$$

The longitudinal force and moment contain contributions from the axial force C_A and the roll-damping coefficients C_{L_p}.

The aerodynamic models shown above represent simple linear aerodynamic models. Nonlinearities in the aerodynamic coefficients exist, typically through a dependence of the aerodynamic coefficients on angle of attack. These effects can be incorporated in the linear aerodyamic model by further expanding the coefficients as functions of the appropriate nonlinearities. As mentioned previously, the virtual wind tunnel model allows the determination of the type of nonlinearity present and allows the proper selection of the functional form to model the nonlinearity. As an example, the axial force in most cases exhibits a quadratic nonlinear dependence on the total angle of attack δ shown below.

$$C_A = C_{A_0} + C_{A_{\delta^2}} \delta^2 \tag{5}$$

For a quadratic nonlinearity, the axial force is represented as a combination of the zero-yaw axial force C_{A_0} and the quadratic yaw axial force $C_{A_{\delta^2}}$.

At a minimum, nine aerodynamic coefficients need to be determined in order to characterize the aerodynamic performance of a projectile, including the six coefficients representing the transverse force and moments, the roll-damping coefficient, and the zero-yaw and quadratic-yaw axial force terms.

VIRTUAL WIND TUNNEL APPROACH

The virtual wind tunnel approach consists of two numerical experiments that are performed to predict the aerodynamic coefficients needed to populate the aerodynamic model shown previously. These two experiments are the Magnus experiment and the pitch-damping experiment. Each Magnus experiment is performed at a fixed angle of attack and spin rate. Typically, predictions are obtained over a range of angles of attack to determine the existence and type of nonlinearities associated with angle of attack. In most applications, only a single nominal spin rate is required because the aerodynamic coefficients appear relatively insensitive to spin rate. The Magnus experiment provides all of the necessary aerodynamics except for the pitch-damping coefficients. The pitch-damping coefficients are obtained from the pitch-damping experiment. At least two approaches for performing the pitch-damping experiment currently exist. These experiments rely on imposed motions to provide the angular rates necessary to produce forces and moments associated with the pitch-damping coefficients. The first approach employs an imposed coning motion to produce the pitch-damping force and moment. Several variants of the coning experiment have been implemented and discussed in the literature. The appropriate selection of the particular type of coning motion depends on the projectile geometry and application. Depending on the geometry and type of coning motion selected, this computation can be performed as a steady-state computation. A second type of pitch-damping experiment can be performed using a simple constant-amplitude sinusoidal pitching motion. This type of experiment must be performed as an unsteady time-accurate computation. Finally, it should be noted that the pitch-damping and Magnus experiments can be combined as a single computation (a spinning projectile undergoing a simple pitching motion or coning motion, for example). However, there appear to be some advantages to performing the two computations independently, especially if nonlinearities are present.

COMPUTATIONAL APPROACH

The virtual wind tunnel approach is a generalized approach and is not necessarily tied to any particular numerical method or computational code. However, the code used to predict the aerodynamic must be capable of performing the two experiments discussed above. In the current computational study, predictions were made with an overset grid approach [2,3] that employs a near-body grid system of interconnecting grids that conform to various parts of the body surrounded by an outer off-body Cartesian-based grid system. The outer off-body Cartesian grid system encompasses the near-body grid system and extends to the outer boundary of the computational domain. The off-body grid system typically consists of several levels of grid refinement, with the most refined grids in proximity to the near-body grids and increasingly less refined grids farther away from the body. The interconnecting near-body and off-body grids overlap and inter-grid connectivity is established using a

Chimera overset gridding approach. The near-body grid system encompassed 78% of the 2.6 million points used for the complete grid.

Solution of the compressible Reynolds-averaged Navier-Stokes equations was accomplished using a three-factor diagonally implicit, first-order accurate time-stepping scheme that employs second-order accurate central differencing in space. The Baldwin-Barth one-equation turbulence model has been used. Characteristics-based inflow/outflow boundary conditions have been applied on the boundaries of the domain. On the body surface, no-slip, adiabatic boundary conditions are imposed.

The Magnus computations were obtained with a simple tangential velocity boundary condition that accounts for the spinning motion of the projectile in a manner that is appropriate for the axisymmetric geometry of the projectiles considered in this study. The pitch-damping experiments were performed with a constant amplitude sinusoidal pitching motion employing an unsteady time-accurate approach. The time-dependent computations were accomplished with a body-fixed oscillating near-body computational mesh that rotates relative to the stationary outer off-body Cartesian grid system. During the course of previous investigations, it was determined that inner iterations at each time step were required to obtain a suitably converged solution for moving grid computations. In the current application, the results seemed less sensitive to the number of inner iterations and typically required fewer than five inner iterations. Five inner iterations were used in the subsequent computational studies. The study also showed that approximately a minimum of a quarter cycle of pitching motion was required to obtain the damping coefficients because of the transients present in starting the solution from a steady constant angle of attack solution.

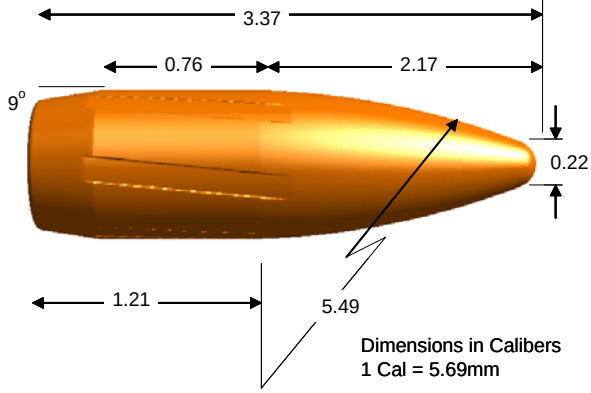

Figure 1. Geometric features of the 5.56mm M193.

RESULTS

A demonstration of the technique was made for the 5.56mm M193 small-caliber projectile shown in Fig. 1. Predictions were made at seven Mach numbers between 1.1 and 3.0 to span the effective range for this projectile. At each Mach number, predictions were made at 0, 2, and 5 degrees to establish the aerodynamic coefficients and to determine the extent of any existing nonlinearities. For this application, this range of angles of

attack was deemed sufficient, although additional angles of attack might need to be considered if significant nonlinearities existed. The predictions were made for standard atmospheric conditions.

From the Magnus experiment, predictions of all the aerodynamic coefficients except for the pitch-damping coefficients were obtained. Predictions of the zero-yaw axial force (Fig. 2) show excellent agreement with the aerodynamic range data. The computations also allowed the typical quadratic yaw drag nonlinearity to be quantified. Both the predictions and spark range data showed a decreasing trend of the quadratic yaw axial force with Mach number, and predictions were within the uncertainty of the data.

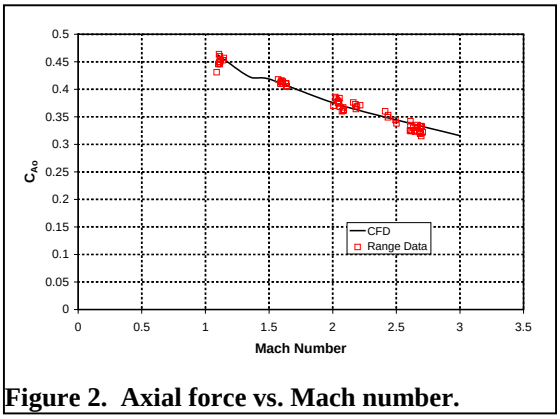

Figure 2. Axial force vs. Mach number.

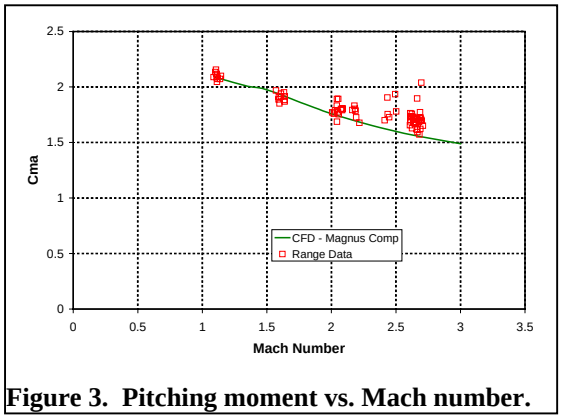

Figure 3. Pitching moment vs. Mach number.

Prediction of the pitching moment coefficient (Fig. 3) also showed excellent agreement with spark range data. Both the pitching moment and normal force revealed little aerodynamic nonlinearity (within a couple percent to 5 degrees angle of attack).

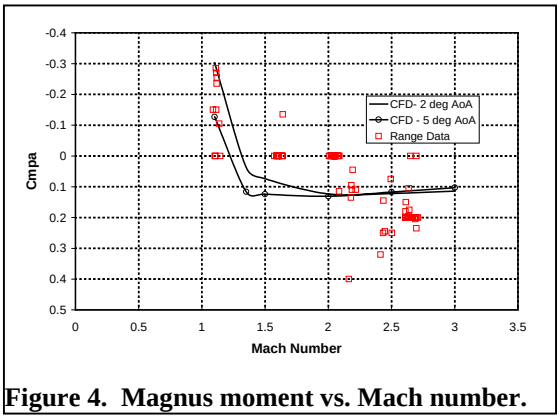

Figure 4. Magnus moment vs. Mach number.

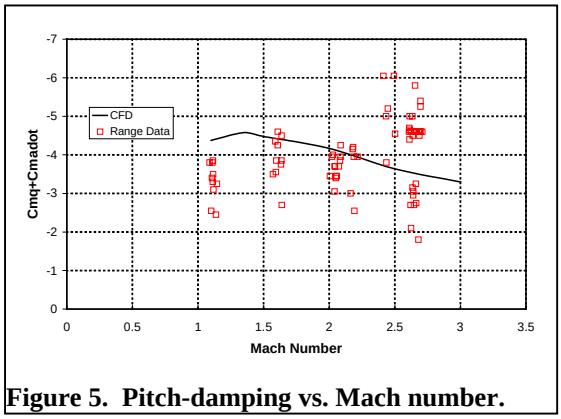

Figure 5. Pitch-damping vs. Mach number.

Figure 4 shows the Magnus moment coefficient versus Mach number for 2 and 5 degrees angle of attack. Here the coefficients are computed are obtained by dividing the moment by the spin rate and angle of attack. The results show a decreasing trend with

Mach number with the Magnus moment becoming negative at some point below Mach 1.5. Below Mach 2.0, some nonlinearity in the results is observed. Examining the force and moment distributions along the body reveals that both the sign change and nonlinear behavior with angle of attack below Mach 2.0 occur near the aft end of the projectile and can be associated with the interaction between the base flow and the after-body geometry. Figure 5 shows the predicted pitch-damping as a function of Mach number compared with the spark range data. The predicted results show the correct trend with Mach number. The scatter in the range data is typical for this type of testing.

Using the computed aerodynamics, the static and dynamic stability of the projectile was assessed. The results show that the projectile, though statically unstable, can be gyroscopically stabilized through the appropriate section of the spin rate. The projectile is also dynamically stable across the expected range of angles of attack and Mach numbers, although weak slow-mode damping and possible instability was observed for small yaw angles at the maximum range of the projectile because of the sign change and nonlinearity in the Magnus moment at the lowest supersonic Mach number. This instability could produce small trim angles that are not uncommon for these types of projectiles.

During the course of the investigation, other projectile geometries were investigated, including the M855. The M855 projectile (Fig. 6) is similar in many respects to the M193, although slightly longer. More significantly, the M855 has a more rounded

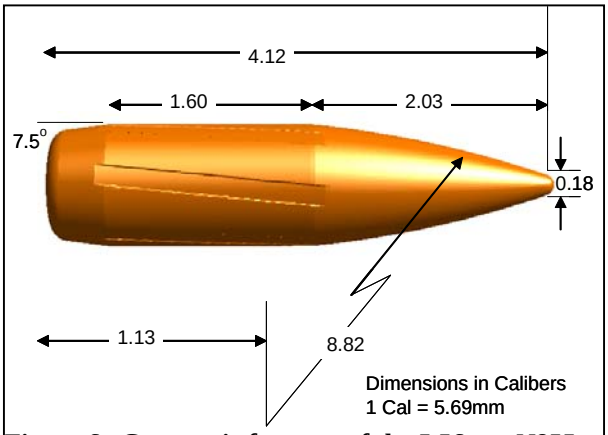

Figure 6. Geometric features of the 5.56mm N855.

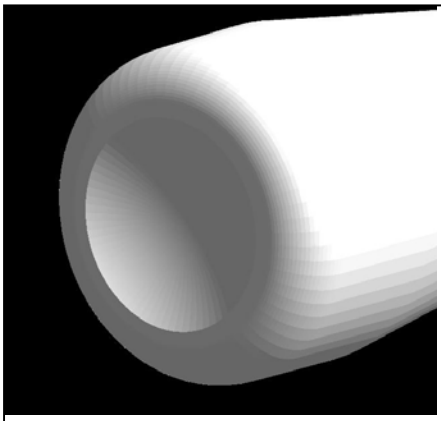

Figure 7. Rounded base corner.

corner at the boattail-base junction (Fig. 7). Application of the virtual wind tunnel technique to the M855 revealed that this geometric feature magnified the nonlinear Magnus behavior of the projectile at low supersonic Mach numbers.

Figure 8 shows the distribution of the Magnus moment along the body at Mach 1.35 for angles of attack between 1 and 5 degrees for the baseline M855 and the M855 with a square base corner. The results show that the rounded base geometry produces a strong

nonlinear Magnus moment variation with angle of attack, and this nonlinearity is confined to the aft portion of the projectile. Modifying the base geometry with a square base geometry virtually eliminates the nonlinearity and produces a sign change in the Magnus moment that is beneficial from a dynamic stability standpoint. Using scientific visualization techniques, it was determined that the asymmetric pressure distribution on the rounded base produced by the interaction of the spin with the asymmetric flow from the angle of attack was responsible for the nonlinear Magnus behavior. Significantly, at moderate supersonic Mach numbers encountered shortly after launch, the pressure on the base region is very low and is unable to generate sufficient force necessary to produce the nonlinear Magnus effect. It is only farther down range where projectile velocity decreases to low supersonic velocities that the base pressure is large enough to produce the nonlinear Magnus effect. Thus, the computational approach was not only able to pinpoint the geometric feature responsible for the effect but was also able to provide a physical rationale for its existence and the flight regime where it should be expected to occur.

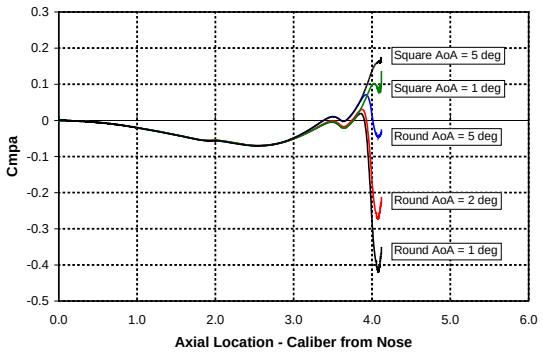

Figure 8. Magnus moment distribution, Mach 1.35.

CONCLUSION

A virtual wind tunnel approach has been applied to examine the aerodynamic performance of small-caliber ammunition. The results for the individual aerodynamic coefficients compare well with spark range data. The results highlight aerodynamic features in the low supersonic regime that can contribute to nonlinear Magnus behavior and trim angles. The results were able to pinpoint the geometric feature responsible for the effect and provide a physical rational for its existence and the flight regime where it should be expected to occur. The technique has also been used to demonstrate the elimination of this behavior through geometric modifications.

REFERENCES

[1] P. Weinacht, “Navier-Stokes Predictions of the Individual Components of the Pitch-Damping Sum,” *Journal of Spacecraft and Rockets*, Vol. 35, No. 5, pp. 598-605, 1998.

[2] K.J. Renze, P.G. Buning, and R.G. Ragagopalan, "A Comparative Study of Turbulence Models for Overset Grids", *AIAA Paper AIAA-92-0437*, January 1992.

[3] R.L. Meakin, "A New Method for Establishing Inter-grid Communication Among Systems of Overset Grids", *AIAA Paper AIAA-91-1586*, June 1991.